

Supporting Information

Hannes Hübener,[†] Umberto De Giovannini,[†] and Angel Rubio^{*,‡,†}

[†]*Max Planck Institute for the Structure and Dynamics of Matter, Luruper Chaussee 149,
22761 Hamburg, Germany.*

*Center for Free-Electron Laser Science and Department of Physics, University of Hamburg,
Luruper Chaussee 149, 22761 Hamburg, Germany*

[‡]*Center for Computational Quantum Physics (CCQ), The Flatiron Institute, 162 Fifth
avenue, New York NY 10010.*

E-mail: angel.rubio@mpsd.mpg.de

Materials and Methods

Computational Details The evolution of the electronic structure under the effect of external fields was computed by propagating the Kohn-Sham (KS) equations in real-space and real time within TDDFT as implemented in the Octopus code.¹ We solved the KS equations in the local density approximation (LDA)² with semi-periodic boundary conditions. We used a simulation box of 60 a_0 along the non-periodic dimension and the primitive cell on the periodic dimensions with a grid spacing of 0.36 a_0 . We modeled graphene with a lattice parameter of 4.651 a_0 and by sampling the Brillouin zone with a 12×12 k-point grid. All calculations were performed using fully relativistic HGH pseudopotentials.³

The linearly polarized phonon mode was prepared by starting the time-evolution of the Kohn-Sham system from a distorted atomic configuration along the C - C bond of 1% of the lattice parameter. From this initial condition the lattice then evolved under Ehrenfest molecular dynamics as a stable oscillatory mode of 20.6 fs, corresponding to an energy of

~ 200 meV. For the circular mode the time-dependence of the lattice was explicitly driven along the circular trajectory corresponding to a superposition of the TO and LO modes with a $\pi/2$ phase difference and with the same frequency as the linear mode. For the photon-excitations with photons shown in Fig. 1 and Fig. 3 the energy was chosen to be same as the phonon energy and the peak intensity was tuned to match the phonon sideband structure with 1.6×10^9 W/cm² for the linearly polarized photons, Fig. 1(b) and Fig. 3(c), and 3.6×10^9 W/cm² for the circularly polarized photons of Fig. 3(d).

Time-resolved ARPES was calculated by recording the flux of the photoelectron current over a surface placed $30 a_0$ away from the system with the t-SURFFP method.⁴ To detect the phonon sideband structure a probe pulse of 50 eV, 80 fs length and a peak intensity of 10^9 W/cm². For Fig. 2(a) a pulse length of 160 fs was used.

The Floquet band structures of the driven system were computed using Floquet-TDDFT⁵ by recording the time-dependent Kohn-Sham Hamiltonians during one cycle of the phonon mode and subsequently performing their Floquet analysis as described in the main text. We found that at least five sidebands were needed to converge the phonon-sideband structure, due to the strong interaction at the Γ point.

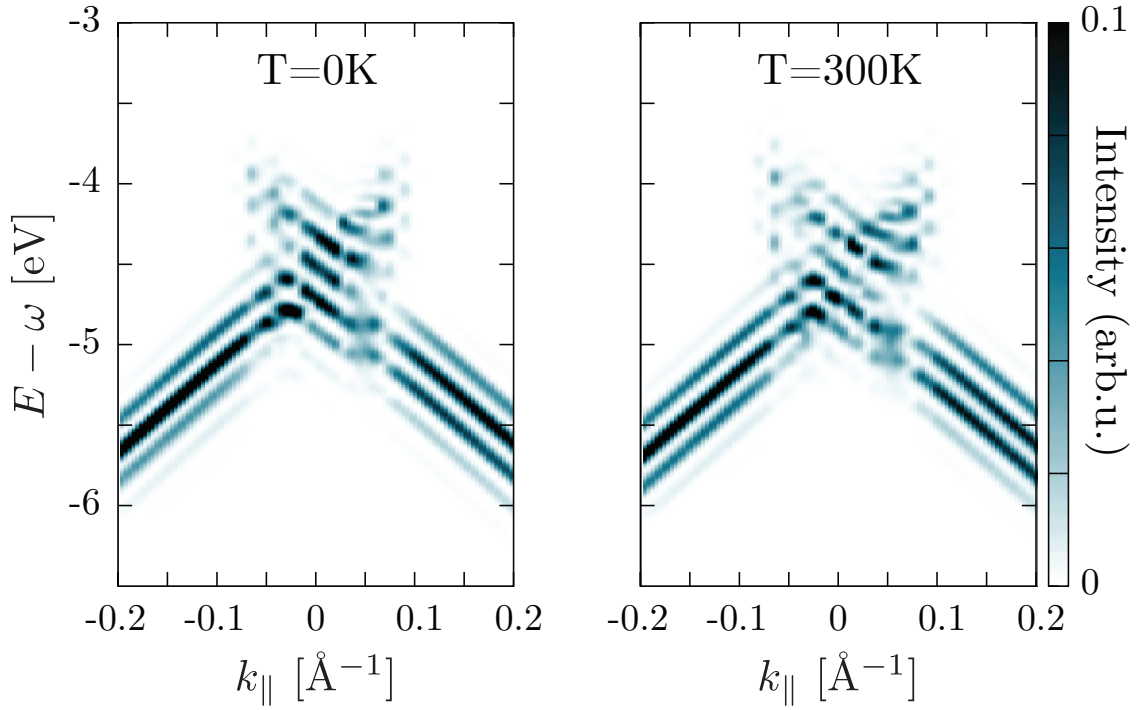


Figure S 1: **Temperature dependence of sideband structure** Tr-ARPES spectrum around the Dirac point with a clean linearly polarized coherent phonon ($T=0\text{K}$) and the same mode under presence of randomized atomic velocities corresponding to a temperature of $T=300\text{K}$.

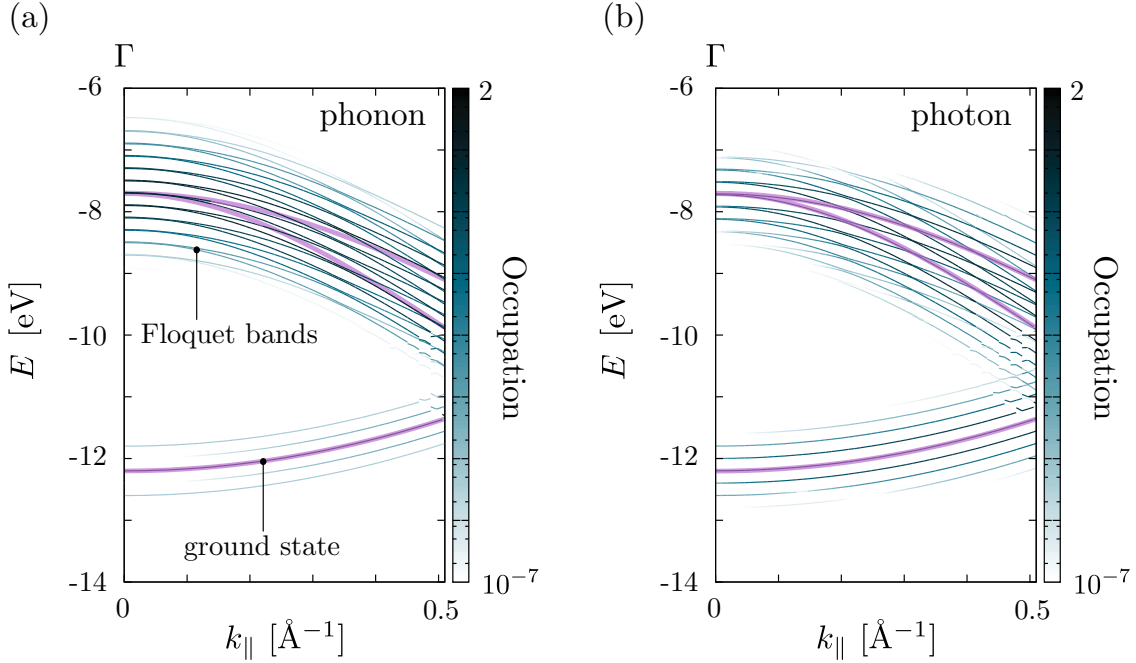


Figure S2: **Floquet-band structure occupation** Occupation of the Floquet-band structure for (a) phonon and (b) photons. The occupation of Floquet-bands are obtained in the sudden approximation.⁶ For a given level $\epsilon_{\alpha}(\mathbf{k})$ this is computed as $f_{\alpha}(\mathbf{k}) = \sum_i |\langle \psi_i(\mathbf{k}) | \Psi_{\alpha}(\mathbf{k}, t) \rangle|^2 f_{\text{FD}}(E_i)$ where the sum runs over all equilibrium states ψ_i with corresponding energies E_i , f_{FD} is the Fermi-Dirac distribution, $\Psi_{\alpha}(\mathbf{k}, t)$ is the time-dependent Floquet eigenstate of level $\epsilon_{\alpha}(\mathbf{k})$ and $\langle \langle . | . \rangle \rangle = 1/T \int_T dt \langle . | . \rangle$ is the scalar product in Floquet space. In purple is shown the equilibrium band structure, showing that the Floquet bands undergo considerable distortion in the phonon case while in the photon case the dressing is trivial in the sense that the occupations decay fast across the sidebands and there is no dispersion dependent deformation of the shifted bands.

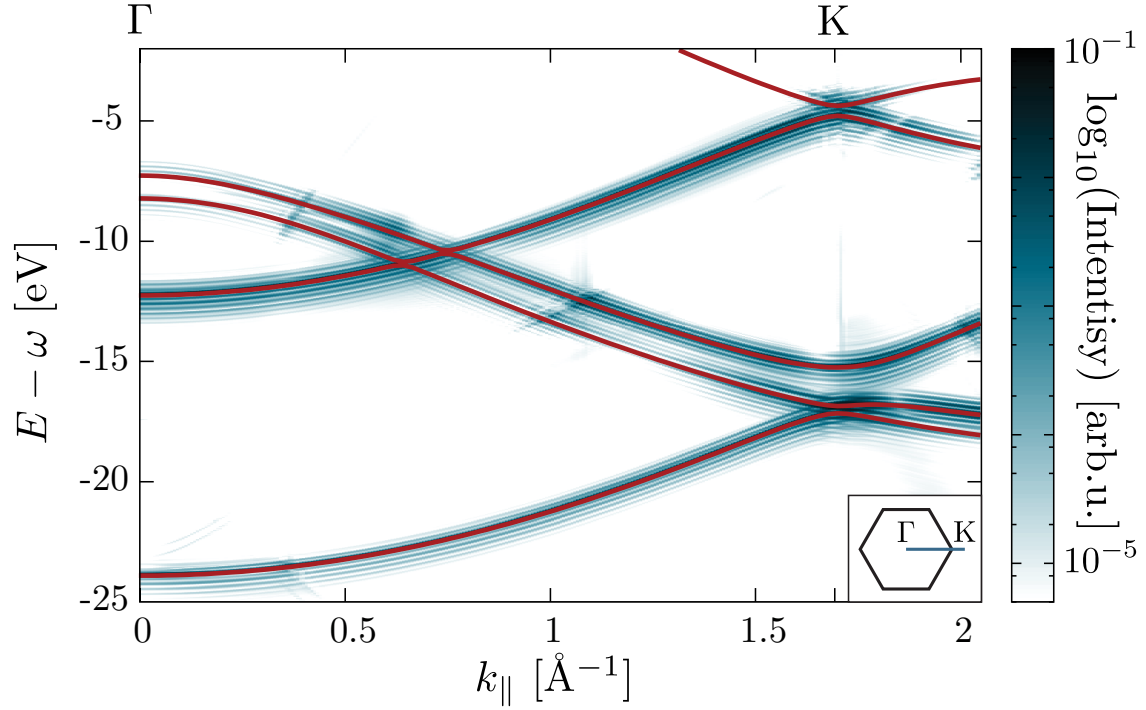


Figure S3: **Floquet sidebands in the first Brillouin zone** Tr-ARPES spectra calculated along a path in the first Brillouin zone. From the spectrum it is clear that the sideband structure is preserved as can be seen comparing with Fig.1 (b) of the main text, the only difference being the photoemission matrix elements reflecting the probability to ionize from a specific Bloch state. The difference is especially striking for the sigma bands close to Γ where the photo-electron signal is suppressed. Note the logarithmic colour scale.

Equivalence of the dynamical excitation with photons and phonons at the Dirac point of graphene The Dirac bands of graphene for Brillouin zone points $\mathbf{k} = (k_x, k_y) = \mathbf{K} - \mathbf{k}'$ around the K -point can be described by the two-level Dirac-Hamiltonian⁷

$$H_{0\mathbf{k}}^D = v_F \boldsymbol{\sigma} \cdot \mathbf{k} = v_F \begin{pmatrix} 0 & k_x - ik_y \\ k_x + ik_y & 0 \end{pmatrix} = v_F |\mathbf{k}| \begin{pmatrix} 0 & e^{-i\theta(\mathbf{k})} \\ e^{i\theta(\mathbf{k})} & 0 \end{pmatrix} \quad (1)$$

where $\boldsymbol{\sigma} = (\sigma_x, \sigma_y)$ is a vector of the in-plane Pauli matrices and $\theta(\mathbf{k})$ is the angle between the \mathbf{k} vector and the x-axis. This Hamiltonian has the eigenstates

$$\psi_{\mathbf{k}}^{\pm}(\mathbf{r}) = \frac{e^{i\mathbf{k} \cdot \mathbf{r}}}{\sqrt{2}} \begin{pmatrix} e^{-i\theta(\mathbf{k})/2} \\ \pm e^{i\theta(\mathbf{k})/2} \end{pmatrix} \quad (2)$$

corresponding to the eigenvalues $E^{\pm} = \pm v_F |\mathbf{k}|$. Coupling to an electro-magnetic field represented by the time-dependent vector potential $\mathbf{A}(t)$ in the weak coupling approximation is done via Peierl's substitution, letting $\mathbf{k} \rightarrow \mathbf{k} - \mathbf{A}(t)$. This gives the light-coupled Dirac Hamiltonian as $H_{\mathbf{k}}^D(t) = v_F \boldsymbol{\sigma} \cdot (\mathbf{k} - \mathbf{A}(t)) = H_{0\mathbf{k}}^D - v_F \boldsymbol{\sigma} \cdot \mathbf{A}(t)$. Writing the vector potential as $\mathbf{A}(t) = (A_x, A_y) \sin(\Omega t)$ from which one can define an angle $\theta(\mathbf{A})$ in analogy to $\theta(\mathbf{k})$ and expanding this Hamiltonian in the eigenbasis of the groundstate, Eq. (2), yields

$$H_{\mathbf{k}}^D(t) = v_F \begin{pmatrix} |\mathbf{k}| & 0 \\ 0 & -|\mathbf{k}| \end{pmatrix} - v_F |\mathbf{A}| \begin{pmatrix} \cos(\theta(\mathbf{k}) - \theta(\mathbf{A})) & -i \sin(\theta(\mathbf{k}) - \theta(\mathbf{A})) \\ i \sin(\theta(\mathbf{k}) - \theta(\mathbf{A})) & -\cos(\theta(\mathbf{k}) - \theta(\mathbf{A})) \end{pmatrix} \sin(\Omega t). \quad (3)$$

The difference between the two angles defines the angle $\theta(\mathbf{k}) - \theta(\mathbf{A}) \equiv \theta_{\mathbf{k}}$ of the main text, i.e. it is the angle between the vector potential and the \mathbf{k} -vector. We note that the interaction matrix corresponds to the dipole matrix elements $m_{ij} \equiv \langle i | \mathbf{p} \cdot \mathbf{A} | j \rangle = \langle i | \partial_{\mathbf{k}} H_{\mathbf{k}}^D | j \rangle = \langle i | \boldsymbol{\sigma} \cdot \mathbf{A}(t) | j \rangle$.

For the phonon perturbation we have to consider a tight-binding representation of the

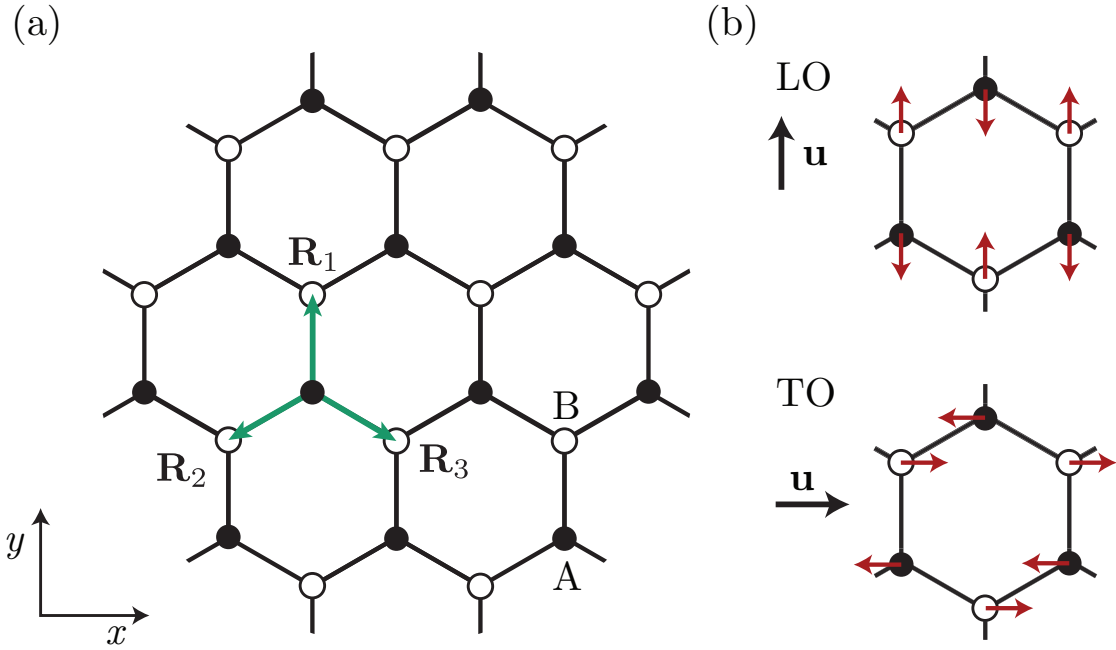


Figure S4: The graphene model used for the tight-binding calculations is shown in (A). The sublattice atoms are labeled A and B . The nearest neighbour vectors \mathbf{R}_a pointing from an A atom to B atoms and are defined as $\mathbf{R}_1 = a_0(0, 1)$, $\mathbf{R}_2 = a_0/2(-\sqrt{3}, -1)$, $\mathbf{R}_3 = a_0/2(\sqrt{3}, -1)$, where a_0 is the C - C bondlength. (b) shows the displacements for the longitudinal (LO) and transverse (TO) modes along with the direction of the phonon polarization \mathbf{u} .

sub-lattice structure of graphene:

$$H_{0\mathbf{k}}^D = -\gamma_0 \sum_{i,a} \left(c_{i+a}^B \right)^\dagger c_i^A + \left(c_i^A \right)^\dagger c_{i+a}^B \quad (4)$$

where A and B are sublattice indices, i runs over all atoms of the sublattice A , a indicates the three nearest neighbours of each A -atom (c.f. Fig. 4) and γ_0 is the effective hopping parameter.⁷ In an on-site sublattice basis this Hamiltonian reads

$$H_{0\mathbf{k}}^D = -\gamma_0 \begin{pmatrix} 0 & f(\mathbf{k}) \\ f(\mathbf{k})^* & 0 \end{pmatrix} \quad (5)$$

where $f(\mathbf{k}) = \sum_a e^{i\mathbf{R}_a \cdot \mathbf{k}}$ and \mathbf{R}_a is the vector connection atom on site A with the nearest neighbour a of the B sublattice. Expanding $f(\mathbf{k})$ around \mathbf{K} gives the Hamiltonian Eq. (1). To first order a coherent phonon mode now has the effect of modifying the lattice hopping term depending on the neighbour index. By writing $H_{\mathbf{k}}^D(t) = H_{0\mathbf{k}}^D + H_{1\mathbf{k}}^D(t)$ we have for the perturbation term

$$H_{1\mathbf{k}}^D(t) = \sum_{i,a} \delta\gamma_0^a(t) \left(c_{i+a}^B \right)^\dagger c_i^A + \left(c_i^A \right)^\dagger c_{i+a}^B. \quad (6)$$

Expanding this again in the sublattice basis and performing that expansion around \mathbf{K} yields⁷

$$H_{1\mathbf{k}}^D(t) = v_F \begin{pmatrix} 0 & A_x^u(t) - iA_y^u(t) \\ A_x^u(t) + iA_y^u(t) & 0 \end{pmatrix} \quad (7)$$

where we have defined $v_F A_x^u(t) = \delta\gamma_0^1(t) - \frac{1}{2}(\delta\gamma_0^2(t) + \delta\gamma_0^3(t))$, $v_F A_y^u(t) = \frac{\sqrt{3}}{2}(\delta\gamma_0^2(t) - \delta\gamma_0^3(t))$ and have assumed that the phonon does not mediate momentum transfer from the lattice to the electron, i.e. we are considering a Γ -point phonon. The coherent phonon can be represented as a time-dependent lattice distortion vector $\mathbf{u}(t)$ which means the hopping term modulations are given as $\delta\gamma^a(t) = g \mathbf{u}(t) \cdot \mathbf{R}_a/a_0$ where g is an effective parameter for the electron-phonon coupling strength. Using the definitions of the nearest neighbour

vectors \mathbf{R}_a , c.f. Fig. S1, one finds $v_F \mathbf{A}^u(t) = g3/2 (u_y(t), -u_x(t))$. This means that the dynamical electron-phonon coupling at the Dirac point of graphene, can be described by the effective gauge field \mathbf{A}^u that is perpendicular to the phonon-mode oscillation vector $\mathbf{u}(t)$, as stated in the main text. Defining the angle $\theta(\mathbf{A}^u)$ one can write Eq. (7) as

$$H_{1\mathbf{k}}^D(t) = g|\mathbf{u}(t)| \begin{pmatrix} 0 & e^{-i\theta(\mathbf{A}^u)} \\ e^{i\theta(\mathbf{A}^u)} & 0 \end{pmatrix} \quad (8)$$

which gives represented in the groundstate eigenbasis, Eq. (2) the form⁸

$$H_{1\mathbf{k}}^D(t) = g|\mathbf{u}(t)| \begin{pmatrix} \cos(\theta(\mathbf{k}) - \theta(\mathbf{A}^u)) & -i \sin(\theta(\mathbf{k}) - \theta(\mathbf{A}^u)) \\ i \sin(\theta(\mathbf{k}) - \theta(\mathbf{A}^u)) & -\cos(\theta(\mathbf{k}) - \theta(\mathbf{A}^u)) \end{pmatrix} \quad (9)$$

which has the same structure as the photon coupling matrix Eq. (3). Thus defining $\theta_{\mathbf{k}} \equiv \theta(\mathbf{k}) - \theta(\mathbf{A}^u)$ as the angle between this effective gauge field and the \mathbf{k} -vector, as well as letting $|\mathbf{u}(t)| = u \sin(\Omega t)$ we have shown that also the coherent phonon coupling leads to a time-dependent Hamiltonian of the form of Eq. (1) of the main text.

References

- (1) Strubbe, D.; De Giovannini, U.; Larsen, A. H.; Varas, A.; Theophilou, I.; Helbig, N.; Verstraete, M. J.; Stella, L.; Aspuru-Guzik, A.; Castro, A. *Physical Chemistry Chemical Physics* **2015**,
- (2) Perdew, J. P. *Physical Review B* **1981**, *23*, 5048–5079.
- (3) Hartwigsen, C.; Goedecker, S.; Hutter, J. *Physical Review B* **1998**, *58*, 3641–3662.
- (4) De Giovannini, U.; Hübener, H.; Rubio, A. *Journal of Chemical Theory and Computation* **2017**, *13*, 265–273.

- (5) Hübener, H.; Sentef, M. A.; De Giovannini, U.; Kemper, A. F.; Rubio, A. *Nature Communications* **2017**, *8*, 13940.
- (6) Oka, T.; Aoki, H. *Journal of Physics: Conference Series* **2011**, *334*, 012060.
- (7) Sasaki, K.-i.; Saito, R. *Progress of Theoretical Physics Supplement* **2008**, *176*, 253–278.
- (8) Pisana, S.; Lazzeri, M.; Casiraghi, C.; Novoselov, K. S.; Geim, A. K.; Ferrari, A. C.; Mauri, F. *Nature Materials* **2007**, *6*, 198–201.